

NUMERICAL SIMULATION OF THE SOLAR THERMAL ENERGY STORAGE SYSTEM FOR DOMESTIC HOT WATER SUPPLY LOCATED IN SOUTH SPAIN

by

**Juan TORRES LEDESMA^{a, b}, Piotr LAPKA^{b*},
Roman DOMANSKI^b, and Francisco S. CASARÉS^a**

^a E.T.S. Ingenieros Industriales, Engineering Building, University of Malaga, Malaga, Spain

^b Institute of Heat Engineering, Warsaw University of Technology, Warsaw, Poland

Original scientific paper
DOI: 10.2298/TSCI111216050L

Nowadays, due to increase in energy consumption, a great deal of fossil fuels is being used. This latter is a consequence of the present environmental problems, such as global warming, acid rain, etc. In order to decrease these problems, the use of renewable energy sources is being promoted. But the renewable energy sources, particularly solar energy, present the drawback that there is a mismatch between the energy demand and supply. To cover this mismatch, the use of phase change thermal energy storage systems is required. In this work, the behaviour of a packed bed latent heat thermal energy storage system co-operating with solar collector located in south Spain was analysed by using a numerical method which based on finite volume discretization and enthalpy method. The model was validated by comparison of the obtained results with experimental data reported in the literature. The packed bed was composed of spherical capsules filled with phase change materials usable for a solar water heating system. The system was designed according to the conditions in the south Spain and by using commercial components available on the market. A series of numerical simulations were conducted applying meteorological data for several months in south Spain, particularly in Malaga.

Key words: *phase change material, thermal energy storage, packed bed, numerical simulation, enthalpy method*

Introduction

Currently, the consumption of energy increases considerably due to technological development and population rise all over the world. Because of this, production and prolongation of energy is the most important problem. Usually, fossil fuels are used as energy sources. However, fossil fuels have some harmful environmental effects on the Earth. All over the world, renewable energy sources are being researched to decrease these effects. Utilization of renewable energy sources can be done together with thermal energy storage (TES) systems. These systems give solutions for the mismatch between the energy demand and supply.

High capacity storage applications can be done with phase change materials (PCM), or also called latent heat storage materials. Waxes, eutectic salt mixtures, and salt hydrates are the most commonly used classes for this purpose, but other type of materials are also considered [1, 2]. The latent heat storage is particularly attractive due to its ability to provide a high energy storage density per unit mass and per unit volume as well as due to its characteristics to store

* Corresponding author; e-mail: piotr.lapka@itc.pw.edu.pl

heat at a constant temperature corresponding to the melting temperature of the PCM. However, practical difficulties usually arise in applying PCM due to its low thermal conductivity, density change during phase change phenomena, stability of properties under extended cycling operation and sometimes phase segregation and subcooling. Therefore, various methods were proposed to enhance the heat transfer in a TES systems. Metallic fillers, metal matrix structures, honeycomb like structures, finned tubes, and aluminum shavings were used to improve thermal conductivity of paraffin [1, 2]. Another method used was to embed the PCM in metal, graphite or carbon foam matrices structure [2, 3]. In order to improve thermal efficiency in several applications the PCM was usually contained in a number of thin flat containers, similar to plate type heat exchangers. Alternatively, it may be contained in small diameter tubes with the heat transfer fluid flowing along or across the tubes [2]. The PCM may also be contained in the wall of a spiral or tube heat exchangers [4]. Another configuration for improving the heat transfer rate was using finned tubes in which the PCM is placed between the fins [5]. In an effort to improve the performance of phase change storage units, the use of more than one PCM with different melting temperatures in a thin flat container was also being suggested [6].

A large improvement in heat transfer performance was also achieved by using small plastic spherical capsules for encapsulating the PCM which can form a packed bed storage unit. The drawbacks of this configuration are the expected high pressure drop through the bed and its initial cost but encapsulation can also solve the problem with changes in a volume during melting or solidification of the PCM [2]. Therefore, this solution is commonly used in the solar TES systems as well as in this work for domestic hot water (DHW) supply. During the charging process, the heat transfer fluid (HTF) from solar collectors flows continuously through the porous bed and the HTF starts to transfer its energy to PCM spherical capsules. Whereas, during the discharging process the energy is released from PCM capsules and is transferred by the HTF to the cold water from the water grid in order to be warmed up and to be used by family as DHW.

Many analytical and numerical methods were developed to describe these packed bed solar TES systems. Ismail and Henriquez [7] presented a numerical model to simulate a storage system with spherical capsules filled with the PCM placed inside a cylindrical tank. They used finite difference approach for modelling fluid and heat flows inside the tank and the moving grid technique for modelling phase change process in PCM capsules. Yuksel *et al.* [8] proposed theoretical approach for prediction of time and temperature during the charging and discharging in the latent heat storage system. Kousksou *et al.* [9] developed a theoretical model for analysis and optimization of the air heating solar collector coupled with TES systems filled with encapsulated PCM. They performed energy and exergy analyses to better understand TES systems behaviour. Hammou and Lacroix [10] proposed a new hybrid TES system for managing the storage of heat from solar collector during days and from electric heater during off-peak periods. They proposed heat transfer model for this TES system and validated it with experimental results. Rady [11] experimentally examined granular phase change composite. Also performances of air TES system with this material for different operating conditions were analysed as well as mathematical model was proposed and was validated with experimental results. Bedecarrats *et al.* [12] numerically modelled an industrial tank filled with encapsulated PCM. They included the supercooling phenomenon and developed mathematical model that enabled investigation of different parameters influences on the behaviour of the tank. Results predicted by the numerical model were compared with experimental values. Regin *et al.* [13] analysed the behaviour of packed bed TES systems filled with spherical capsules with PCM usable with solar water heating system. They applied model similar to the Schumann model.

As approximately from 20% to 25% of the annual expenses in a house is spent in the production of DHW, the TES system application in houses is economically justified. However, utilization of TES systems needs carefully analysis which depends on the climate zone and the local weather condition. Analyses for particular regions and climate conditions were not very common in the literature. Additionally, TES systems investigated in the others papers did not consist of elements that were available on the market. Therefore the purpose of this work was to create a simple tool that enables to simulate working cycle of solar TES systems with encapsulated PCM for DHW with application of appropriated meteorological data for the specific region. The analysed system was composed of commercial elements that might be found on the market. The propose numerical tool could be also helpful in selection of optimal elements and operating conditions of TES systems. Working cycle of solar TES systems was simulated by applying finite volume discretization and enthalpy method for the phase change phenomena. The model was validated with experimental results available in [14]. Consequently, numerical analyses were performed for the TES system filled with encapsulated PCM and in co-operation with solar collectors for DHW supply in a single-family house located in the city of Malaga (south Spain).

Modelled unit description

The schematic diagram of the system under study, which is shown in fig.1, consisted of an insulated cylindrical TES tank containing PCM encapsulated spherical capsules, an evacuated solar collector, two circulating pumps, a hot water accumulator, and the DHW outer system. The $D = 300$ mm diameter and $H = 570$ mm height stainless steel TES tank had a capacity of 40 litres. These values were obtained by energy analysis to the whole system (hot water demand for 4 person family: 120 litres per day at 60 °C; average grid water temperature 15.5 °C; bed porosity 0.32) and by taking into account a ratio between the diameter and length of the TES tank that should be around 1.75 and 2 [15]. The hot water accumulator had a capacity of 80 litres to supply hot water for a family of 4 persons, with a daily DHW demand of 120 litres. There were two plenum chambers on the top and on the bottom of the tank and a flow distributor was provided on the top of the tank to achieve uniform flow of HTF. The storage tank was insulated with 50 mm thick glass wool.

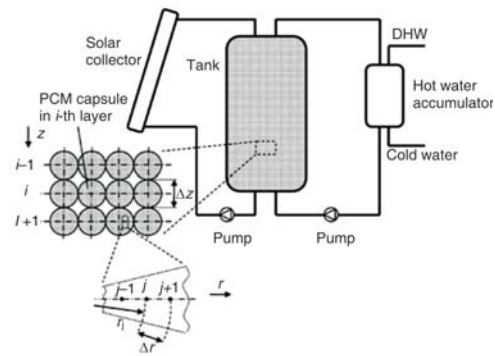


Figure 1. Scheme of the TES system under consideration

For the selection of the $A_{col} = 2$ m² solar collector, obtained from the requirements specified in the national technical building code [15], characteristics of durability and performance were taken into account. The selected solar collector was an evacuated solar collector because of its high performance compared with solar plate collectors. It belonged to the manufacturer THERMOMAX and its characteristics are shown in tab. 1.

Table 1. Collector characteristics

Manufacturer	Model	η_0 [-]	k_1 [Wm ⁻² K ⁻¹]	k_2 [Wm ⁻² K ⁻¹]	\dot{m} [l min ⁻¹]	α/ε [-]	A_{col} [m ²]
THERMOMAX	DF100-2 m	83.0	1.53	0.0063	2.0-3.0	95/5	2.0

The HTF was a mixture of water and propylene glycol, with a composition of this latter one equal to 13% in mass. This proportion of propylene glycol was calculated according to the meteorological data, particularly, by using the historical lowest temperature in Malaga, which was $-4\text{ }^{\circ}\text{C}$. The HTF will transfer the energy to $D_{\text{ext}} = 50\text{ mm}$ outer diameter of the spherical capsules, size obtained from the average of diameters used in [13, 16-21], which was made of high-density polyethylene with wall thickness of $R_{\text{ext}} - R_{\text{int}} = 0.8\text{ mm}$. Paraffin, from the manufacturer *PCM PRODUCTS*, was used as PCM inside the spherical capsules with a melting temperature equal to $T_m = 62\text{ }^{\circ}\text{C}$, due to the fact that the melting temperature must be situated between the outlet collector temperature and the operation temperature for DHW [22], recommended to be $60\text{ }^{\circ}\text{C}$ by the Technical Building Code [15]. Other parameters of the PCM were: thermal conductivity in the liquid and solid phases of $k_{\text{PCM}} = 0.3\text{ W/mK}$, a specific heat of $c_{p,\text{PCM}} = 1900\text{ J/kgK}$ in the solid phase and of $c_{p,\text{PCM}} = 2200\text{ J/kgK}$ in the liquid phase and latent heat of fusion of $L_{\text{PCM}} = 202\text{ kJ/kg}$. The spherical capsules were uniformly packed in $M_f = 7$ layers through the tank, each supported by wire mesh. The void fraction or porosity of tank was $\varepsilon = 0.32$. This means that PCM spherical capsules occupied 67.5% of the storage tank total volume and the remaining was occupied by the sensible heat storage material which was HTF. The mass flow rate was set according to the solar collector manufacturer recommendations and its value for loading and for the unloading processes was $\dot{m} = 160\text{ kg/h}$. The 8 mm diameter copper pipes between the evacuated solar collector and the TES system and between this latter one and the hot water accumulator were insulated with a thermal conductivity coefficient of 0.04 W/mK material. The thickness of the insulation was calculated to be 20 mm .

Mathematical formulation

The mathematical model, which describes the behaviour of the TES system combined with solar collectors, presented in fig. 1, is subjected to the following assumptions.

- The tank and all pipes in the TES system were fully insulated.
- The flow at a constant mass flow rate was laminar, axial, incompressible, and Newtonian.
- Constant velocity in a cross-section of the tank was assumed, so fluid temperature was varying only in axial direction.
- The Rayleigh number for liquid PCM in the capsule was very small due to small capsule radius, high molten PCM viscosity and small temperature difference in the capsule, therefore convection in the liquid PCM was neglected.
- The heat flux on the capsule surface was constant. Therefore, temperature and liquid fraction inside the PCM capsule were varying only in radial direction.
- Thermophysical properties of the HTF and the PCM were temperature independent.
- Supercooling or superheating in the PCM was not considered.

Based on these assumptions, energy conservation equations for the HTF in the axisymmetric co-ordinate system and for the encapsulated PCM in the spherical co-ordinate system can be written as:

$$\varepsilon \rho_f c_{p,f} \left(\frac{\partial T_f}{\partial t} + u \frac{\partial T_f}{\partial z} \right) = \frac{\partial}{\partial z} \left(k_{\text{ef}} \frac{\partial T_f}{\partial z} \right) + UA_c N [T(r = R_{\text{int}}) - T_f] \quad (1)$$

$$\rho_{\text{PCM}} c_{p,\text{PCM}} \frac{\partial T}{\partial t} = \frac{1}{r^2} \frac{\partial}{\partial r} \left(k_{\text{PCM}} r^2 \frac{\partial T}{\partial r} \right) - \rho_{\text{PCM}} L_{\text{PCM}} \frac{\partial f}{\partial t} \quad (2)$$

where the effective thermal conductivity of the HTF k_{ef} is used due to high turbulence in the flow field and is defined as [16]:

$$k_{\text{ef}} = 0.5 \text{ Re}_f \text{ Pr}_f k_f \quad (3)$$

The Re_f can be obtained from the definition: $Re_f = \rho_f u D_{ext} / \mu_f$, where the superficial velocity u in the porous bed equals to $u = \dot{m} / \varepsilon \rho_f A$ and A is the tank cross-section area. This expression is valid for $Re_f > 0.8$. The second term on the right hand side of eq. (1) represents the heat exchanged between the HTF and the N spherical capsules filled with PCM for i -th layer of porous bed. The global heat transfer coefficient U through the shell of capsule times the capsule area A_c can be calculated by applying thermal resistance method (fig. 2):

$$UA_c = \left[\frac{1}{4\pi R_{ext}^2 h_c} + \frac{R_{ext} - R_{int}}{4\pi k_s R_{ext} R_{int}} \right]^{-1} \quad (4)$$

The external convective heat transfer coefficient h_c was calculated from an empirical correlation for Nu proposed by Beek [23]. This correlation is valid for big diameter spherical particles layer of cubic arrangement suitable for energy storage applications and for $Re_f > 40.0$:

$$Nu_f = 2.42 \sqrt[3]{Re_f} \sqrt[3]{Pr_f} + 0.129 Re_f^{0.8} Pr_f^{0.4} + 1.4 Re_f^{0.4} \quad (5)$$

Constant HTF temperature in the tank equal to temperature of water from water grid system and equal to final temperature after heat accumulation were taken as initial conditions for charging and discharging processes, respectively. During heating process the temperature of HTF $T_f(z=0, t)$ at tank inlet depends on amount of a solar energy absorbed by solar collectors $Q_s(t)$ as well as the outlet tank temperature $T_f(z=H, t)$, and was calculated applying balance of energy for solar collector:

$$T_f(z=0, t) = T_f(z=H, t) + \frac{Q_s(t)}{\dot{m} c_p} \quad (6)$$

The time dependent solar energy absorbed by the collector $Q_s(t)$ takes the form:

$$Q_s(t) = A_{col} \int_0^t G(t) \eta(t) dt \quad (7)$$

where the solar collector efficiency $\eta(t)$ was obtained from the relationship (tab. 1):

$$\eta(t) = \eta_0 - k_1 \frac{[T_f(z=h, t) - T_a(t)]}{G(t)} - k_2 \frac{[T_f(z=h, t) - T_a(t)]^2}{G(t)} \quad (8)$$

The global solar radiation intensity $G(t)$ and ambient temperature $T_a(t)$ were varying during the day and were taken according to meteorological data for south Spain.

During discharging process the HTF inlet temperature, T_{ini} , was constant and equals to the temperature of water from water grid system. At the exit of the tank the boundary condition had a form:

$$\frac{\partial T_f}{\partial z_{z=H}} = 0 \quad (9)$$

For the PCM inside the capsule following boundary conditions were adopted:

$$\frac{\partial T}{\partial r_{r=0}} = 0 \quad (10)$$

$$\frac{-k_{PCM} \partial T}{\partial r_{r=R_{int}}} = UA_c [T(r=R_{int}) - T_f] \quad (11)$$

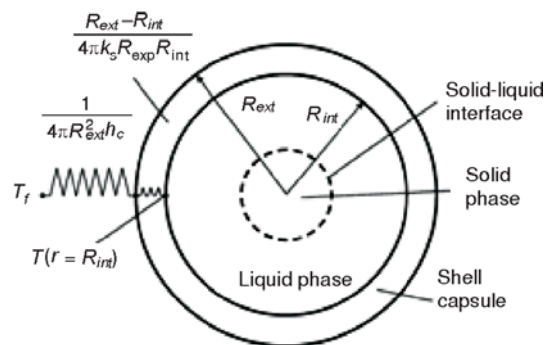


Figure 2. Scheme of a capsule with PCM

Numerical solution

The energy equation for working fluid, eq. (1) was discretized applying the finite volume method (FVM) [24, 25]. This method offers the advantage that the solution obtained satisfies the conservation of mass, momentum, and energy, regardless of the number of nodes used. It bases on dividing the domain under study in a finite number of non-overlapping control volumes, so that within each control volume there is a central node at which the unknown temperature is calculated. The tank under consideration filled with packed bed column was divided into number of elements which equals to number of PCM capsules layers M_f in the tank. These elements had size Δz equal to the external diameter of capsule $\Delta z = D_{\text{ext}}$, as it is presented in fig. 1. The time derivative was discretized using fully implicit forward scheme. For diffusion term second order central differencing scheme was used, whereas for convection term upwind differencing scheme was applied. The final discrete equation for HTF for all internal nodes was in the form:

$$\begin{aligned} & \varepsilon \rho_f c_{p,f} \frac{T_{f,i}^{k+1} - T_{f,i}^k}{\Delta t} + \varepsilon \rho_f c_{p,f} u (T_{f,i}^{k+1} - T_{f,i-1}^{k+1}) = \\ & = \left(k_{\text{ef},i+1} \frac{T_{f,i+1}^{k+1} - T_{f,i}^{k+1}}{\Delta z} - k_{\text{ef},i-1} \frac{T_{f,i}^{k+1} - T_{f,i-1}^{k+1}}{\Delta z} \right) + UA_c N (T_{M_{\text{PCM}}}^{k+1} - T_{f,i}^{k+1}) \Delta z \end{aligned} \quad (12)$$

For the PCM capsule Eulerian, fixed grid enthalpy method [25, 26] and FVM [24, 25] with an implicit forward time scheme and second order central differencing special scheme were applied. The capsule was divided into M_{PCM} elements of size Δr as schematically shown in fig. 1. Finally, following discrete form of energy equation inside the PCM, eq. (2), for all internal nodes was obtained:

$$\begin{aligned} & \left[\frac{k_{\text{PCM}} r_{j+1}^2}{\Delta r} + \left(\frac{r_{j+1} + r_{j-1}}{2} \right)^2 \rho_{\text{PCM}} c_{p,\text{PCM}} \frac{\Delta r}{\Delta t} + \frac{k_{\text{PCM}} r_{j-1}^2}{\Delta r} \right] T_j^{k+1} - \\ & - \frac{k_{\text{PCM}} r_{j+1}^2}{\Delta r} T_{j+1}^{k+1} - \frac{k_{\text{PCM}} r_{j-1}^2}{\Delta r} T_{j-1}^{k+1} = \left(\frac{r_{j+1} + r_{j-1}}{2} \right)^2 \rho_{\text{PCM}} c_{p,\text{PCM}} \frac{\Delta r}{\Delta t} T_j^k - \\ & - \left(\frac{r_{j+1} + r_{j-1}}{2} \right)^2 - \rho_{\text{PCM}} L_{\text{PCM}} \Delta r \frac{f_j^{k+1} - f_j^k}{\Delta t} \end{aligned} \quad (13)$$

Equations (12) and (13) were modified at boundary nodes in order to fulfill boundary conditions. The evolution of the liquid fraction was determined iteratively from formula [25, 26]:

$$f_j^{k+1} = f_j^k + \omega \frac{\frac{k_{\text{PCM}} r_{j+1}^2}{\Delta r} + \left(\frac{r_{j+1}^2 + r_{j-1}^2}{2} \right) \rho_{\text{PCM}} c_{p,\text{PCM}} \frac{\Delta r}{\Delta t} + \frac{k_{\text{PCM}} r_{j-1}^2}{\Delta r}}{\left(\frac{r_{j+1} + r_{j-1}}{2} \right)^2 \rho_{\text{PCM}} L_{\text{PCM}}} (T_j^k - T_m) \frac{\Delta t}{\Delta r} \quad (14)$$

The liquid fraction calculated from eq. (14) should be corrected in each iteration as follows:

$$f_j^{k+1} = \begin{cases} 0 & \text{for } f_j^{k+1} < 0 \\ 1 & \text{for } f_j^{k+1} > 1 \end{cases} \quad (15)$$

The calculations were conducted iteratively. The overall solution procedure is presented in fig. 3. Implicit systems of eqs. (12) and (13) with proper boundary conditions, were solved by using the Gaussian elimination algorithm with partial pivoting instead of using the inverse algorithm, as this later one has a computational cost of (n^3) operations instead of (n^2) operations for the Gaussian algorithm.

Validation

In order to prove the credibility of the developed mathematical model, a comparison between the numerical predictions for the fourth layer $i = 4$ and the experimental data reported in [14] was carried out. The thermophysical properties as well as operating and geometrical parameters were taken according to [14]. As it can be observed in fig. 4, the agreement between experimental and numerical results was reasonable. It can be noticed that in the numerical results the PCM reached its melting temperature faster than in the experimental one. This was assumed to be due to the basic assumptions made in the mathematical model of the fluid that the conduction resistance of the tank was neglected, which means, that there were no thermal losses through the tank and pipes. From the same figure, it can be observed that the calculated PCM melting time was slightly longer than the experimental one, which may be due to the fact that the natural convection within the liquid PCM was ignored. Another reason that may explain the difference of the PCM temperature for solid phase was the use of constant properties, regardless of the temperature.

Results

Distributions of the temperature in the medium ring of the sphere filled with PCM in the fourth layer $i = 4$ were calculated for the representative days of several months in Spain. This position represents the average temperature through the sphere. The months were those, firstly, in which the climatic conditions were

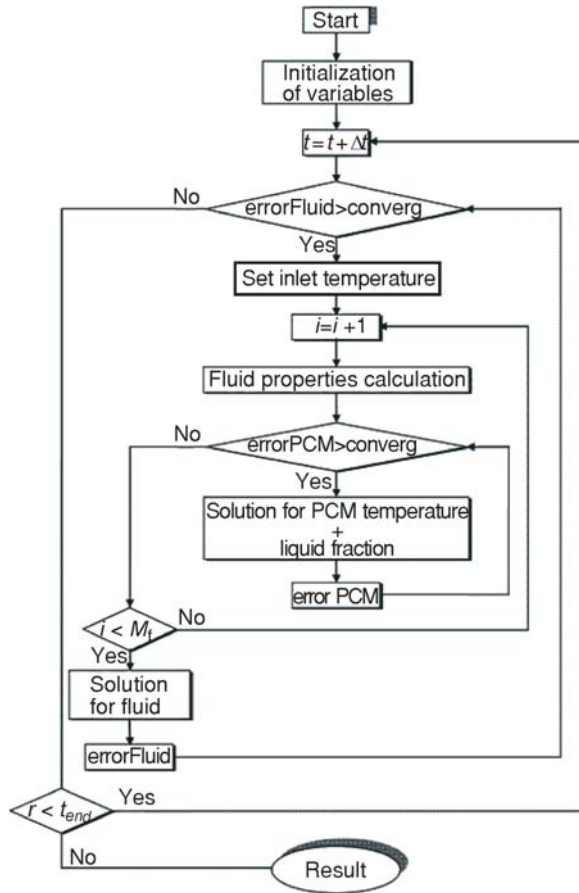


Figure 3. The overall solution procedure scheme

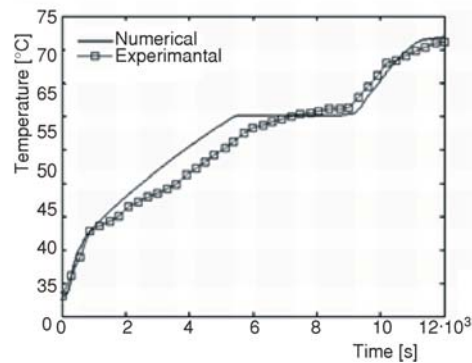


Figure 4. Comparison between numerical and experimental results

extreme, that means, those months in which the highest and lowest values of irradiation were recorded and secondly those months between both extremes ones with average conditions. Therefore April, July, September, and December were taken during calculation as the most representative.

In a first approximation and in order to make the calculations, the boundary condition for the temperature at the inlet to the tank was chosen as the outlet solar collector temperature (eq. 6), neglecting on this way the thermal and pressure losses in the pipe which connects these elements. This temperature was represented by a sinusoidal-like function, which was span between hours when the Sun starts to irradiate collector until the highest air temperature was reached. This later one corresponds to 14:00, 14:00, 13:00, and midday within April, July, September, and December, respectively. In tabs. 2 and 3 the average ambient temperature and the average solar irradiation during the Sun hours for Malaga as well as the water grid average temperature were shown, respectively, for the months commented previously. These data were obtained by applying a free software AMT provided by the Autonomous Community of Andalusia. The aim of AMT is the generation of the extreme meteorological data for the different towns of Andalusia as well as the visualization, manipulation, and exportation of the hourly data of the provincial capitals of Andalusia.

Table 2. Average ambient temperature and average solar irradiation during sun hours for different months for Malaga

Hour	April		July		September		December	
	T_a [°C]	G [Wm ⁻²]						
5:00-6:00	10.5	–	20.4	304	17.3	–	7.1	–
6:00-7:00	10.9	30	21.0	421	17.9	378	7.5	–
7:00-8:00	11.5	103	21.8	599	18.6	487	7.8	23
8:00-9:00	12.7	284	23.0	707	19.8	652	8.1	188
9:00-10:00	14.3	548	24.5	792	21.7	750	9.6	448
10:00-11:00	16.1	705	26.2	855	23.6	820	11.6	625
11:00-12:00	18.0	742	27.6	894	25.6	862	13.6	754
12:00-13:00	19.5	848	29.3	906	27.2	877	15.5	801
13:00-14:00	20.6	935	30.3	894	28.5	862	16.8	754
14:00-15:00	21.0	798	30.5	855	29.4	820	17.5	625
15:00-16:00	20.6	637	30.5	792	29.4	750	17.5	448
16:00-17:00	20.0	431	29.8	707	28.5	652	16.6	188
17:00-18:00	19.0	184	28.8	599	27.0	487	15.3	23
18:00-19:00	17.6	52	27.5	421	25.2	378	14.8	–
19:00-20:00	16.8	–	26.0	304	23.9	–	14.0	–

Table 3. Water grid average temperature for different months for Malaga

Month	April	July	September	December
Water grid average temperature [°C]	13	16	14	8

Figures 5-8 represent the distribution of temperature for the medium ring of the PCM sphere for December, April, July and September, respectively. Moreover in July, for being the most representative month, the distribution of the melting fraction during the loading process and the distribution of the temperature for the medium ring during the unloading process were presented in figs. 9 and 10, respectively.

In December, as it can be noticed in fig. 5, the TES system did not work as it was desired, as the temperature of the PCM in the medium ring did not reach the melting temperature. Thus, the DHW must be heated in the boiler in order to leave the system at 60 °C. Nevertheless,

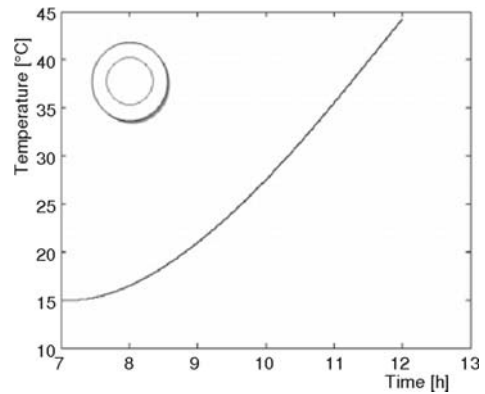


Figure 5. PCM medium ring temperature distribution for the loading process in December

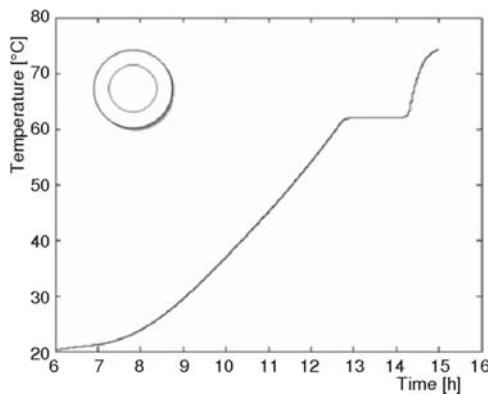


Figure 6. PCM medium ring temperature distribution for the loading process in April

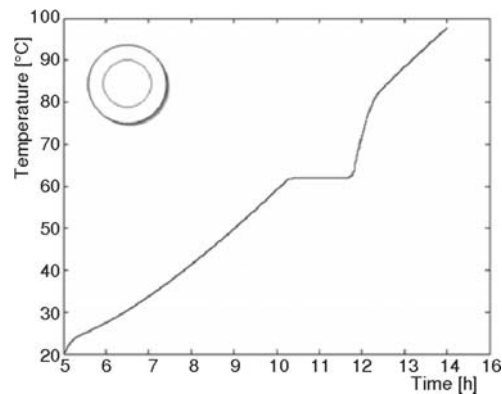


Figure 7. PCM medium ring temperature distribution for the loading process in July

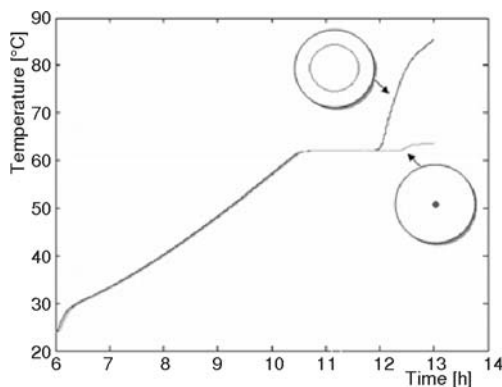


Figure 8. PCM medium ring and centre temperature distribution for the loading process in September

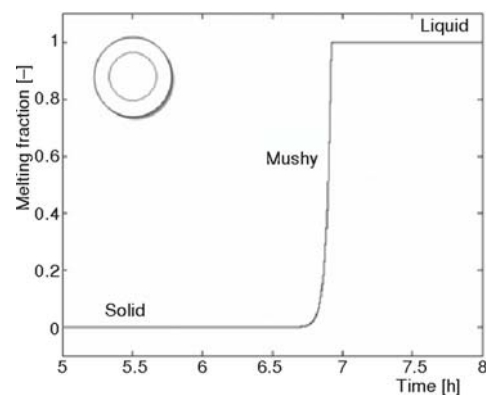


Figure 9. PCM medium ring melting fraction for the loading process in July

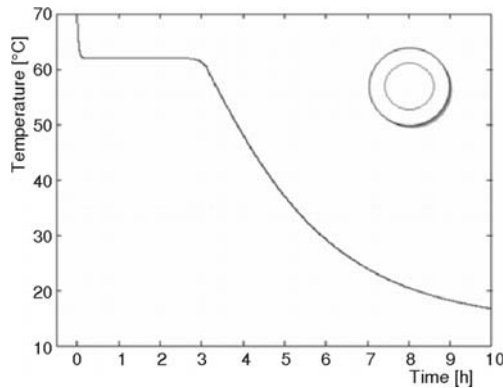


Figure 10. PCM medium ring temperature distribution for the unloading process in July

zones of the PCM was shown in the medium ring and in the centre. The behavior of both lines is almost the same for solid phase of PCM and during the phase change, but it changes in the liquid phase. In this phase, the temperature distribution for the centre undergoes a smoother increase than in the medium ring. Therefore, it can be concluded that the distance from the surface affects to the distribution of the temperature over the time.

Conclusions

In this paper a numerical model of TES systems filled with encapsulated PCM co-operating with solar collectors for DHW supply in a single-family house was presented. This model can be applied for modelling operating cycles of the solar TES system taking into account the climate zone and local weather condition for particular regions of the world. The model could be also helpful in optimal selection of elements and operating conditions for solar TES systems. Therefore, the whole system was composed of elements that can be found on the market. These elements were chosen according to design recommendations [15]. The model was validated against the experimental data [14]. Furthermore, some numerical analyses were performed for Malaga (south Spain) applying the meteorological data for most representative month *i. e.* April, July, September, and December. The presented model was subjected to several assumptions. Some of them should be relaxed in the future work to better simulate real systems.

Acknowledgment

Piotr Lapka acknowledges financial support from the European Union in the framework of European Social Fund through the Didactic Development Program of the Faculty of Power and Aeronautical Engineering of the Warsaw University of Technology.

Nomenclature

A, A_c	– tank cross-section, PCM capsule, [m ²]	H	– tank height, [m]
A_{col}	– solar collector area, [m ²]	k	– thermal conductivity, [Wm ⁻¹ K ⁻¹]
c_p	– specific heat, [Jkg ⁻¹ K ⁻¹]	k_1, k_2	– thermal drop coefficients, [Wm ⁻² K ⁻¹]
D, D_{ext}	– tank diameter, capsule external diameter, [m]	L	– latent heat of fusion, [Jkg ⁻¹]
f	– liquid fraction, [–]	M_f	– numbers of layers in the tank, [–]
h_c	– convective heat transfer coefficient, [Wm ⁻² K ⁻¹]	M_{PCM}	– numbers of elements in PCM capsule, [–]
G	– global solar radiation intensity, [Wm ⁻²]	\dot{m}	– mass flow rate, [kgs ⁻¹]
		N	– numbers of capsules in the layer, [–]

this latter behavior changes during the other months, see figs. 6-8. For instance in July, the PCM temperature was around 100 °C. So, the HTF might be warm to a higher temperature, close to the boiling point. In the reality this behavior must be avoided by using a control system. In April, see fig. 6, and in September, see fig. 8, the PCM reached almost the same temperature, but the loading time was slightly higher in September than in April. Regarding July, see figs. 7 and 10, it can be noticed that the unloading time during the phase change was approximately twice the loading time.

In September, as it can be observed in fig. 8,

Nu	– Nusselt number ($= h_c D_{\text{ext}}/k$), [–]	ε	– bed porosity, emissivity, [–]
Pr	– Prandtl number ($= c_p \mu/k$), [–]	η, η_0	– solar collector efficiency, solar collector optical parameter, [–]
$R_{\text{int}}, R_{\text{ext}}$	– internal, external capsule radius, [m]	μ	– dynamic viscosity, [Pa·s]
r	– radius, [m]	ρ	– density, [kgm^{-3}]
r, z	– radial, axial co-ordinates, [m]	ω	– under relaxation factor, [–]
Re	– Reynolds number ($= \rho u D_{\text{ext}}/\mu$), [–]	Subscripts	
t	– time, [s]	f	– heat transfer fluid
T, T_a, T_f	– PCM, ambient, fluid temperature, [°C]	PCM	– phase change material
T_m	– melting temperature, [°C]	s	– shell
Δt	– time step, [s]	ini	– initial
u	– superficial velocity, [ms^{-1}]	i, j	– indices
U	– total heat transfer coefficient, [$\text{Wm}^{-2}\text{K}^{-1}$]	Superscripts	
$\Delta r, \Delta z$	– PCM, fluid meshsize, [m]	k	– time level
Greek symbols			
α	– absorptivity, [–]		

References

- [1] Hasnain, S. M., Review on Sustainable Thermal Energy Storage Technologies, Part I: Heat Storage Materials and Techniques, *Energy Conversion and Management*, 39 (1998), 11, pp. 1127-1138
- [2] Zalba, B., *et al.*, Review on Thermal Energy Storage with Phase Change: Materials, Heat Transfer Analysis and Applications, *Applied Thermal Engineering*, 23 (2003), 3, pp. 251-283
- [3] Mesalhy, O., *et al.*, Carbon Foam Matrices Saturated with PCM for Thermal Protection Purposes, *Carbon*, 44 (2006), 10, pp. 2080-2088
- [4] Banaszek, J., *et al.*, Experimental Study of Solid-Liquid Phase Change in a Spiral Thermal Energy Storage Unit, *Applied Thermal Engineering*, 19 (1999), 12, pp. 1253-1277
- [5] Domanski, R., *et al.*, Numerical Analysis of Heat Transfer in PCM Containers Embedded in Heat Sinks for Electronics Cooling, *Proceedings*, 5th International Conference on Transport Phenomena In Multiphase Systems, Bialystok, Poland, 2008, vol. 2, pp. 167-174
- [6] Shaikh, S., Lafdi, K., Effect of Multiple Change Materials (PCM) Slab Configurations on Thermal Energy Storage, *Energy Conversion and Management*, 47 (2006), 15-16, pp. 2103-2117
- [7] Ismail, K. A. R., Henriquez, J. R., Numerical and Experimental Study of Spherical Capsules Packed Bed Latent Heat Storage System, *Applied Thermal Engineering*, 22 (2002), 15, pp. 1705-1716
- [8] Yuksel, N., *et al.*, A Model for Latent Heat Energy Storage Systems, *International Journal of Energy Research*, 30 (2006), 14, pp. 1146-1157
- [9] Kousksou, T., *et al.*, Second Law Analysis of Latent Thermal Storage for Solar System, *Solar Energy Materials and Solar Cells*, 91 (2007), 14, pp. 1275-1281
- [10] Hammou, Z. A., Lacroix, M., A Hybrid Thermal Energy Storage System for Managing Simultaneously Solar and Electric Energy, *Energy Conversion and Management*, 47 (2006), 3, pp. 273-288
- [11] Rady, M., Granular Phase Change Materials for Thermal Energy Storage: Experimental and Numerical Simulations, *Applied Thermal Engineering*, 29 (2009), 14-15, pp. 3149-3159
- [12] Bedecarrats, J. P., *et al.*, Study of a Phase Change Energy Storage Using Spherical Capsules, Part II: Numerical Modelling, *Energy Conversion and Management*, 50 (2009), 10, pp. 2537-2546
- [13] Regin, A. F., *et al.*, An Analysis of a Packed Bed Latent Heat Thermal Energy Storage System Using PCM Capsules: Numerical Investigation, *Renewable Energy*, 34 (2009), 7, pp. 1765-1773
- [14] Nallusamy, N., *et al.*, Study on Performance of a Packed Bed Latent Heat Thermal Energy Storage Unit Integrated with Solar Water Heating System, *Journal of Zhejiang University SCIENCE A*, 7 (2006), 8, pp. 1422-1430
- [15] ***, Technical Building Code, <http://www.codigotecnico.org>
- [16] Ismail, K. A. R., Stuginsky Jr., R., A Parametric Study on Possible Fixed Bed Models for PCM and Sensible Heat Storage, *Applied Thermal Engineering*, 19 (1999), 7, pp. 757-788
- [17] Sari, A., Form-Stable Paraffin/High Density Polyethylene Composites as Solid-Liquid Phase Change Material for Thermal Energy Storage: Preparation and Thermal Properties, *Energy Conversion and Management*, 45 (2004), 13-14, pp. 2033-2042

- [18] Kousksou, T., *et al.*, Numerical Simulation of Fluid Flow and Heat Transfer in a Phase Change Thermal Energy Storage, *International Journal of Energy Technology and Policy*, 6 (2008), 1, pp. 143-158
- [19] Cho, K., Choi, S. H., Thermal Characteristics of Paraffin in a Spherical Capsule During Freezing and Melting Processes, *International Journal of Heat and Mass Transfer*, 43 (2000), 17, pp. 3183-3196
- [20] Levent, B., Zafer, I., Total Solidification Time of a Liquid Phase Change Material Enclosed in Cylindrical/Spherical Containers, *Applied Thermal Engineering*, 25 (2005), 10, pp. 1488-1502
- [21] Ismail, K. A. R., Moraes, R. I. R., A Numerical and Experimental Investigation of Different Containers and PCM Options for Cold Storage Modular Units for Domestic Applications, *International Journal of Heat and Mass Transfer*, 52 (2009), 19-20, pp. 4195-4202
- [22] Mehling, H., Cabeza, F. L., *Heat and Cold Storage with PCM: An Up to Date Introduction into Basic and Applications*, Springer-Verlag, Berlin, 2008
- [23] Beek, J., Design of Packed Catalytic Reactors, *Advances in Chemical Engineering*, 3 (1962), pp. 203-271
- [24] Versteeg, H. K., Malalasekera, W., *An Introduction to Computational Fluid Dynamics. The Finite Volume Method*, Pearson, Harlow, N. D., USA, 2007
- [25] Lapka, P., Furmanski, P., Numerical Modelling of Solidification Processes of Semitransparent Materials Using the Enthalpy and the Finite Volume Methods, *Heat and Mass Transfer*, 44 (2008), 8, pp. 937-957
- [26] Voller, R. V., Fast Implicit Finite-Difference Method for the Analysis of Phase Change Problems, *Numerical Heat Transfer Part B*, 17 (1990), 2, pp.155-169